GA–A24321

MODELING OF EBW COUPLING WITH WAVEGUIDE LAUNCHERS FOR NSTX

by
R.I. PINSKER, G. TAYLOR, and P.C. EFTHIMION

MAY 2003

GENERAL ATOMICS

DISCLAIMER

GA–A24321

MODELING OF EBW COUPLING WITH WAVEGUIDE LAUNCHERS FOR NSTX

by
R.I. PINSKER, G. TAYLOR,* and P.C. EFTHIMION*

This is a preprint of a paper to be presented at the 15th Topical Conference on Radio Frequency Power in Plasmas, Moran,Wyoming, May 19–21, 2003 and to be published in the *Proceedings.*

*Princeton Plasma Physics Laboratory, Princeton, New Jersey.

Work supported by
the U.S. Department of Energy
under Grant No. DE-FG03-99ER54522
and Contract DE-AC02-76CH03073

GENERAL ATOMICS PROJECT 30041
MAY 2003

GENERAL ATOMICS

Modeling of EBW Coupling with Waveguide Launchers for NSTX

R.I. Pinsker, G. Taylor,[a] and P.C. Efthimion[a]

General Atomics, P.O. Box 85608, San Diego, California 92186-5608
[a]Princeton Plasma Physics Laboratory, Princeton, NJ 08543

Abstract. The theory originally developed for the MST EBW waveguide coupling experiments [1] is used to model coupling to the EBW in the National Spherical Torus eXperiment (NSTX).

Numerous recent papers have described the coupling between electron Bernstein waves (EBWs) in the plasma interior and waves that can propagate in vacuum (O- and X-modes). This topic is of interest both for electron cyclotron emission diagnostics in overdense plasmas and for possible high-power heating methods appropriate to such overdense plasmas as are characteristic of reversed-field pinches and spherical torii. In this paper, we apply the theory developed for the Madison Symmetric Torus (MST) EBW waveguide coupling experiments [1,2] to the case of NSTX, using parameters for NSTX taken from Ref. [3].

The coupling theory developed in Refs. [1] and [2] is an application of the Brambilla "grill" theory in the lower hybrid range of frequencies [4] to the range of electron cyclotron harmonics. A weakly collisional cold-plasma model is used. Just as in the theory of Ram, et al. [5], the resulting reflection coefficients are nearly identical to those obtained with a full kinetic plasma model, in which the EBW appears explicitly. The difference is that the energy that is absorbed near the upper hybrid resonance (UHR) layer by the weak collisions in the cold plasma model is instead converted to inward-propagating EBWs in the full kinetic description. This has been checked by comparing the surface admittances obtained using this cold plasma model with those computed by the GLOSI code [6], which includes the lowest order EBW in the model. Excellent agreement is found in all cases, verifying the basic assumption of the model.

The program embodying this model has two parts: 1) the calculation of the surface admittances as functions of n_y and n_z, and 2) the calculation of all of the integrals convolving these admittances with the appropriate spectral functions for a phased array of identical rectangular waveguides operating in the fundamental mode. The results of those integrals then yield the reflection coefficients and the amplitudes of the first few evanescent modes in each of the waveguides in the array for an arbitrary excitation (phasing). First, we check the analytic theory results given by Ram for the 'straight-in' case (n_y=n_z=0) using only the first part of the program.

We take f = 11.6 GHz, and we assume a purely toroidal field with B(x) = (4 kG)(85 cm)/[85 cm + 67 cm – x (cm)]. We assume the following form of the density profile in the extreme edge region: $n(x) = (3\times10^{12}\ \mathrm{cm}^{-3})\ \exp[(x-g)/L_n]$ for $0 < x < x_{end}$, and in the nominal case, we take L_n = 0.7 cm, g = 1.5 cm, x_{end} = 1.7 cm. The density profile and the locations of the cutoffs and UHR are shown in Fig. 1. The solid curve is the nominal (L_n = 0.7 cm) density profile, while the nearly horizontal dashed lines represent the densities at which R=0 (right-hand cutoff), S=0 (UHR), and L=0 (left-hand cutoff). To keep all of the other physics. To keep all of the other physics constant as the gradient scale-length L_n is varied, the "gap" g is adjusted to keep the position of the UHR fixed at x = 0.83 cm, and x_{end} is adjusted so that the density at x_{end} is constant. The other curves in the figure show a few of the resulting family of density profiles with different values of L_n, one with much shorter L_n and two with shallower gradients.

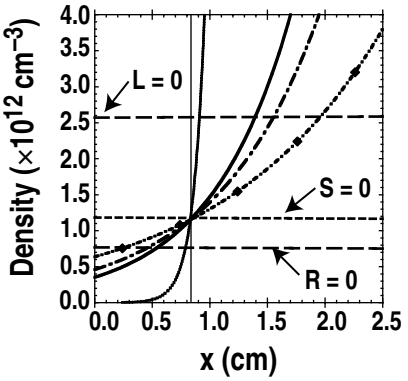

Figure 1. Density profiles for scan of gradient at UHR for NSTX.

For the straight-in case, the translation of the surface admittance to a reflection coefficient $|\rho|^2$ is straightforward. In the case where the calculation ends at a density higher than the L=0 cutoff, there is no energy propagation to larger x possible in the cold plasma model, so that the power mode-conversion coefficient is just $1 - |\rho|^2$. The mode-conversion coefficient thus computed as a function of the gradient scale length is shown in Fig. 2 as the solid curve. Also, we compute the same quantity for these profiles, except x_{end} is chosen such that the slow X-mode is still propagating at the high density boundary of the calculation zone. The resulting $1 - |\rho|^2$ is shown as the dashed curve with superimposed ×symbols. This case corresponds to the classic Budden problem, with the right-hand cutoff and the UHR, as opposed to the "triplet resonator" case. In the Budden problem, $1 - |\rho|^2$ does not correspond to the power mode converted at the UHR, since energy can propagate out of the calculational zone on the slowX-branch. In the limit of extremely short L_n, there is no reflected wave, and all of the power is transmitted to the slow X-mode branch. Therefore, the quantity $1 - |\rho|^2$ goes to 1 as L_n goes to zero, but the mode-conversion coefficient also goes to 0.

Also in Fig. 2, the numerical full-wave solutions are compared with the analytic theories given by Ram for those two cases, as well as to the experimental data given in Ref. [3]. The analytic estimate which is compared with the experimental data in Ref. [3] does not appear to be reproduced by the numerical solution. The numerical result for the transmission coefficient does not exceed about 80% even at the optimum value of L_n, and there is no sign of oscillations due to the interference between the forward and reflected waves between the UHR and L=0 layers. The simple formula for the quantity $1 - |\rho|^2$ in the Budden case (solid line with no symbols) reproduces the numeric results rather well, and in the range of L_n so far accessed experimentally there is not much difference between the Budden case and the full triplet case. The optimum

gradient is significantly steeper than the setup of that preliminary experiment permitted.

All of these calculations so far have considered only the single plane wave with $n_y=n_z=0$. But the work in Refs.[1] and [2] has shown that there is a very strong effect of non-zero n_y in these parameter ranges. This effect is the same one that, in a much lower frequency range, causes the asymmetry in FW antenna loading between co- and counter-current phasing [8]. Mathematically, the effect is a result of the terms in the wave equation involving the products of n_y and spatial derivatives of the off-diagonal element of the dielectric tensor. These terms are dropped in the WKB approximation, and they are first order in n_y and in the gradient of the off-diagonal tensor element, K_{xy}, or D in Stix's notation. This means that the effect depends on the sign of n_y and on the sign of D. These non-WKB terms are most important exactly when the gradient is steep compared to the X-mode wavelength, which in this case means for L shorter than a few centimeters. Even for values of L_n much longer than this, these terms are still important as long as an UHR layer is present in the coupling zone, since these terms all diverge as S vanishes.

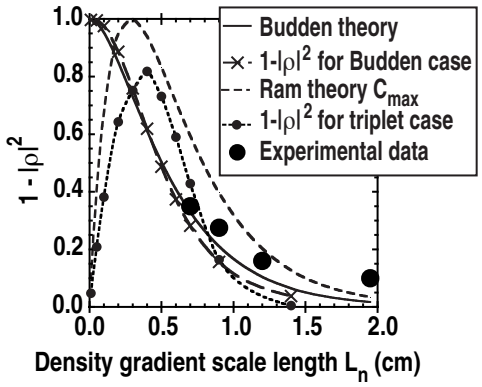

Figure 2. Comparison of numerical full wave solutions for "straight-in" propagation with approximate analytic formulas.

For a discontinuous ("step") density profile, a unidirectional surface wave [2] propagates in the y-direction in the plane of the discontinuity. When a continuous density profile is assumed, what was a true surface wave in the step profile case becomes a very slowly penetrating wave. As the density gradient decreases, then the distance from the right-hand cutoff to the upper hybrid layer increases and the amplitude of the fields to excite the UHR becomes low. Hence, the distance that the slowly penetrating wave must propagate along the y-direction before the power is absorbed (again, really mode-converted) at the upper hybrid becomes large.

We next consider the simplest possible n_y-specific launcher and apply our code to compute the reflection coefficients for NSTX-like parameters. We take the same rf and plasma parameters as in the single plane wave calculations, and we take the launcher to consist of a pair of vacuum waveguides stacked poloidally, of opening dimensions 2.2 cm along the static magnetic field and 1.1 cm vertically. Note that the Brambilla-type models do not model the situation where a waveguide is protruding some distance above a ground plane; in that situation, currents on the top and bottom surfaces of the waveguide tend to make the guide more directive than with a ground plane.

First, the phasing between the forward waves in the two guides is set at zero, to most nearly approximate the single "straight-in" plane wave case, and we compute the reflection coefficient in the guides as a function of the assumed gradient scale length. The resulting transmission coefficient is shown as the solid line in Fig. 3. The transmission coefficient has much less variation with L_n on the shallow gradient side than

in the "straight-in" plane wave case. This is a result of the rather efficient excitation of the surface-wave-like mode, propagating nearly poloidally in one direction. The maximum transmission coefficient is obtained by phasing the guides so that the peak of the excited spectrum coincides with the maximal excitation of that mode. The dashed line with the superimposed × symbols shows the transmission coefficient obtained at the optimum poloidal phasing angle, and the remaining dashed curve with the filled circles shows the poloidal phase angle at which that optimum is achieved. The transmission coefficient remains above 80% for all gradient scale lengths greater than about 2 mm. However, the poloidal localization of the start of the EBW propagation would be expected to get less well defined the larger the value of L_n.

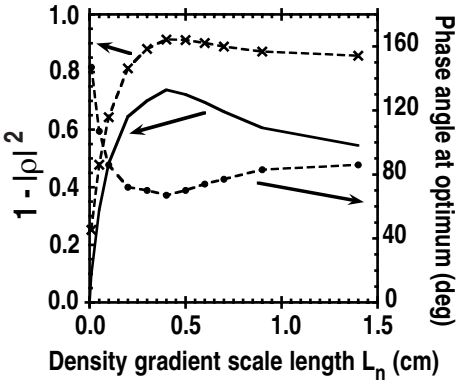

Figure 3. Transmission coefficient for two waveguide array coupler for in-phase operation, operation at the optimal y-phasing, and the phase angle for which that optimum is obtained for NSTX conditions.

The combination of local limiters to reduce the value of L_n with some poloidal phasing would probably result in such a low reflection coefficient that the poloidal phasing could be fixed at a value of 75 or 80 degrees, instead of the relatively complicated system necessary to make that phasing adjustable. The limiters would not be expected to strongly interact with the launched waves, since the launched wave would primarily go 'up' or 'down' depending on the sign of the toroidal field and the corresponding phasing, while the limiters are separated in the toroidal (horizontal) direction.

ACKNOWLEDGMENT

Work supported by the U.S. Department of Energy under Grant DE-FG03-99ER54522 and Contract DE-AC02-76CH03073.

REFERENCES

[1] Pinsker, R.I., et al., "Calculation of Direct Coupling to the Electron Bernstein Wave With a Waveguide Antenna," *Proc. 14th Top. Conf. on RF Power in Plasmas*, edited by T.K. Mau and J.S. deGrassie, AIP Conference Proceedings, Oxnard, 2001, p. 350.
[2] Pinsker, R.I., et al., "Calculation of Coupling to the Electron Bernstein Wave With a Phased Waveguide Array," submitted to *Plasma Phys. Control. Fusion* (2003).
[3] Taylor, G., *Phys. Plasmas* **10**, 1395 (2003).
[4] Brambilla, M.., *Nucl. Fusion* **16**, 47 (1976).
[5] Ram, A.K. and Schultz, S., *Phys. Plasmas* **7**, 4084 (2000).
[6] Wang, C.Y., et al., *Phys. Plasmas* **2**, 2760 (1995).
[7] Ram, A.K. et al., *Phys. Plasmas* **3**, 1976 (1996).
[8] Jaeger, E.F., *Nucl. Fusion* **38**, 1 (1998).